# Optimal Nodal Flyby with Near-Earth Asteroids Using Electric Sail

Giovanni Mengali, Alessandro A. Quarta *

*Department of Civil and Industrial Engineering, University of Pisa, I-56122 Pisa, Italy*

**Abstract**

The aim of this paper is to quantify the performance of an Electric Solar Wind Sail for accomplishing flyby missions toward one of the two orbital nodes of a near-Earth asteroid. Assuming a simplified, two-dimensional mission scenario, a preliminary mission analysis has been conducted involving the whole known population of those asteroids at the beginning of the 2013 year. The analysis of each mission scenario has been performed within an optimal framework, by calculating the minimum-time trajectory required to reach each orbital node of the target asteroid. A considerable amount of simulation data have been collected, using the spacecraft characteristic acceleration as a parameter to quantify the Electric Solar Wind Sail propulsive performance. The minimum time trajectory exhibits a different structure, which may or may not include a solar wind assist maneuver, depending both on the Sun-node distance and the value of the spacecraft characteristic acceleration. Simulations show that over $60\%$ of near-Earth asteroids can be reached with a total mission time less than $100\,\mathrm{days}$, whereas the entire population can be reached in less than ten months with a spacecraft characteristic acceleration of $1\,\mathrm{mm/s^2}$ .

*Key words:* Electric Solar Wind Sail, NEA exploration, trajectory optimization.

* Corresponding author.
*Email addresses:* g.mengali@ing.unipi.it (Giovanni Mengali), a.quarta@ing.unipi.it (Alessandro A. Quarta).

**Nomenclature**

| | | |
|---|---|---|
| $a_c$ | = | spacecraft characteristic acceleration |
| $a_\oplus$ | = | Earth's orbit semimajor axis |
| $e_\oplus$ | = | Earth's orbit eccentricity |
| $\mathcal{H}$ | = | Hamiltonian function |
| $\mathcal{J}$ | = | set of NEAs |
| $r$ | = | Sun-spacecraft distance ($r_\oplus \triangleq 1\,\text{au}$) |
| $\mathcal{T}(r,\theta)$ | = | polar reference frame |
| $t$ | = | time ($t_f$ is the total flight time) |
| $v$ | = | spacecraft velocity modulus |
| $\alpha$ | = | sail cone angle |
| $\alpha_\lambda$ | = | reference angle, see Eq. (12) |
| $\theta$ | = | polar angle |
| $\lambda_i$ | = | adjoint to variable $i$ |
| $\mu_\odot$ | = | Sun's gravitational parameter |
| $\nu$ | = | true anomaly |
| $\tau$ | = | switching parameter |

*Subscripts*

| | | |
|---|---|---|
| 0 | = | initial |
| $f$ | = | final, target |
| $r$ | = | radial |
| $\theta$ | = | transverse |
| max | = | maximum |

*Superscripts*

$\dot{}$ = time derivative

$\bar{}$ = mean value over $\nu_0$

## 1 Introduction

The interest of the scientific community in studying Near Earth Asteroids (NEAs) is emphasized by the increasing number of papers that have been devoted to this matter, especially in the last decade. A detailed review about NEAs and their possible threat to our planet, including an up-to-date and extensive bibliography, is given in the recent review paper by Perna et al. [1] to which the interested reader is referred for further information. After the pioneering successes of the American mission Near Earth Asteroid Rendezvous – Shoemaker [2] and the more recent conclusion of Japanese Hayabusa mission [3,4], the two proposed European missions Don Quijote [5] and Marco Polo [6,7] are expected to represent a fundamental step forward in the knowledge of these interesting celestial bodies of the Solar System.

In general terms, an orbital rendezvous with a NEA using a robotic mission is a rather involved problem, due to the typical non-negligible orbital inclination of those (minor) celestial bodies [8,9] . For example, about 49% of the currently known NEAs (that is, over 9500 asteroids at the beginning of the 2013 year), have a heliocentric orbital inclination greater than 10 deg. Such a characteristic, especially when coupled with a non-negligible value of orbital eccentricity, in most cases requires the need of a large $\Delta V$ to perform a classical rendezvous mission with an high-thrust propulsion system as, for example, a chemical rocket. A substantial reduction of the necessary $\Delta V$ can be obtained by relaxing the constraints regarding the terminal phase of the mission, for example by performing a close encounter with the asteroid instead of

an orbital rendezvous. Within the context of flyby missions toward NEAs, Ref. [10] discusses an interesting approach, referred to as nodal flyby, in which the target asteroid is reached at one of its two orbital nodes using an impulsive transfer. A similar idea has been subsequently exploited in Ref. [11] to accomplish a preliminary mission analysis toward long-period comets with high orbital inclination and using a photonic solar sail, that is, a spacecraft with a propellantless (primary) propulsion system that provides a continuous, low, propulsive acceleration. For example, Table 6 of Ref. [11] shows that the flight time required to reach the descending node of comet Hale-Bopp ranges between about 200 and 660 days depending on the photonic solar sail performance.

The aim of this work is to apply the nodal flyby concept to a mission analysis using a spacecraft whose propulsion system is constituted by an Electric Solar Wind Sail (E-Sail) [12,13]. The E-sail is an innovative propulsion concept, which uses the solar wind dynamic pressure for generating a propulsive acceleration without the need for reaction mass. As such, it represents an interesting option for robotic missions toward NEAs, especially when a small scientific payload mass is considered [14].

In this paper all NEAs in the set of known asteroids (evaluated at mid-January 2013) have been considered as potential targets in a robotic mission scenario. The analysis of each mission case has been performed within an optimal framework, by calculating the minimum-time trajectory necessary to reach one orbital node of the target asteroid. This amounts to finding the optimal mission performance irrespective of the initial and final E-sail positions at both the parking orbit and the target node. The use of such a simplified mission scenario, in which the ephemeris constraints are not taken into account, is a common choice in a preliminary mission analysis [15], and is necessary to accomplish a thorough investigation involving the whole population of NEAs with reasonable simulation times. For each target the optimal problem has been solved with an indirect approach, using different values of the spacecraft characteristic acceleration. The mathematical model, which is briefly described in the next section, has been

adapted from that discussed in Ref. [15].

As a result of the study, a database with the outputs of nearly 19 000 optimal transfers has been created. In this sense, this work is an extension of a previous paper [16] presented at the 7th Symposium On Realistic Advanced Scientific Space Missions (Aosta, 2011) and completes the analysis of Ref. [15] regarding an E-sail based mission towards potentially hazardous asteroids. The collected simulation data are sufficient for obtaining a first order estimation of the performance required by an E-sail to fulfil a mission toward a NEA.

## 2 Mathematical Model

According to the most recent studies [12], the E-sail propulsive acceleration modulus depends on the Sun-spacecraft distance $r$ as $a_c\,(r_\oplus/r)$, where $a_c$ is the spacecraft characteristic acceleration, that is, the maximum propulsive acceleration at a reference distance $r_\oplus \triangleq 1\,\mathrm{au}$.

Assuming a two-dimensional transfer, the heliocentric equations of motion for an E-sail in an ecliptic polar reference frame $\mathcal{T}_\odot(r,\theta)$ are (see Fig. 1):

$$\dot{r} = v_r \tag{1}$$

$$\dot{\theta} = \frac{v_\theta}{r} \tag{2}$$

$$\dot{v}_r = \frac{v_\theta^2}{r} - \frac{\mu_\odot}{r^2} + a_c\,\tau\,\frac{r_\oplus}{r}\,\cos\alpha \tag{3}$$

$$\dot{v}_\theta = -\frac{v_r\,v_\theta}{r} + a_c\,\tau\,\frac{r_\oplus}{r}\,\sin\alpha \tag{4}$$

where the polar angle $\theta$ is measured anticlockwise from the Sun-spacecraft position at the beginning of the transfer phase, the thrust angle $\alpha \in [-\alpha_{\max}, \alpha_{\max}]$ coincides with the angle between the Sun-spacecraft line and the thrust direction, $\alpha_{\max}$ is the maximum cone angle (in this paper it is assumed that $\alpha_{\max} = 30\,\mathrm{deg}$, see Ref. [15]), and the switching parameter

$\tau = (0, 1)$ models the E-sail on/off condition.

The following analysis is performed assuming a circular Earth's heliocentric orbit and an E-sail deployment on a parabolic Earth escape trajectory, that is, with zero hyperbolic excess energy with respect to the planet. The latter is a common assumption that is usually adopted to obtain conservative results and to reduce the number of free parameters in the problem. The other assumption of circular Earth's orbit guarantees a remarkable simplification of the analytical model as well as a substantial complexity reduction in the solution of the two-point boundary value problem associated to the minimum time problem. However, the numerical simulations have shown that the actual eccentricity of the terrestrial orbit has a negligible effect on the optimal flight time unless the characteristic acceleration takes very small values. In the latter case the corresponding flight time would be very long and the E-sail would not represent a feasible propulsive option.

For example, assuming a characteristic acceleration of $a_c = 1\,\mathrm{mm/s^2}$, Fig. 2 shows the transfer time $t_f$ as a function of the final distance $r_f$ and of the starting true anomaly $\nu_0 \in [0,\, 360]\,\mathrm{deg}$ when the true eccentricity of the terrestrial orbit is taken into account ($e_\oplus = 0.01671022$ and $a_\oplus = 1.00000011\,\mathrm{au}$). Note that the flight time is normalized with its mean value $\bar{t}_f$, the latter being calculated with respect to the starting true anomaly $\nu_0$. The values of $\bar{t}_f$ are shown in Table 1 as a function of $r_f \leq 12\,\mathrm{au}$ . Figure 2 confirms that the variation of the flight time with the starting spacecraft position is indeed negligible. Figure 2 is split into two parts, showing separately what happens for $r_f < 1\,\mathrm{au}$ and $r_f > 1\,\mathrm{au}$ and, for readability reasons, the latter is confined to not exceed $5\,\mathrm{au}$ .

Returning to the case of circular Earth's orbit, the spacecraft initial state (at time $t_0 \triangleq 0$) is (see also Fig. 1)

$$r(t_0) = r_\oplus \quad , \quad \theta(t_0) = 0 \quad , \quad v_r(t_0) = 0 \quad , \quad v_\theta(t_0) = \sqrt{\mu_\odot / r_\oplus} \tag{5}$$

The problem is to find the minimum time (optimal) trajectory necessary to reach a prescribed distance $r_f = r(t_f)$, where $t_f$ is the flight time to be minimized. The optimal control law is obtained with an indirect approach in which the Hamiltonian function is

$$\mathcal{H} \triangleq \lambda_r\, v_r + \lambda_\theta\, \frac{v_\theta}{r} + \lambda_{v_r} \left( \frac{v_\theta^2}{r} - \frac{\mu_\odot}{r^2} \right) - \lambda_{v_\theta}\, \frac{v_r\, v_\theta}{r} + a_c\, \tau\, \frac{r_\oplus}{r}\, (\lambda_{v_r}\, \cos\alpha + \lambda_{v_\theta}\, \sin\alpha) \tag{6}$$

where $\lambda_i$ is the adjoint variable associated with the state variable $i$. The time derivatives of adjoint variables are given by the Euler-Lagrange equations:

$$\dot{\lambda}_r = \frac{\lambda_\theta\, v_\theta}{r^2} + \lambda_{v_r} \left( \frac{v_\theta^2}{r^2} - \frac{2\,\mu_\odot}{r^3} \right) - \lambda_{v_\theta}\, \frac{v_r\, v_\theta}{r^2} + \frac{a_c\, \tau\, r_\oplus}{r^2}\, (\lambda_{v_r}\, \cos\alpha + \lambda_{v_\theta}\, \sin\alpha) \tag{7}$$

$$\dot{\lambda}_\theta = 0 \tag{8}$$

$$\dot{\lambda}_{v_r} = -\lambda_r + \lambda_{v_\theta}\, \frac{v_\theta}{r} \tag{9}$$

$$\dot{\lambda}_{v_\theta} = -\frac{\lambda_\theta}{r} - 2\, \frac{\lambda_{v_r}\, v_\theta}{r} + \frac{\lambda_{v_\theta}\, v_r}{r} \tag{10}$$

Using the Pontryagin maximum principle, and according to Ref. [17], the optimal steering law that maximizes the Hamiltonian function is:

$$\alpha = \begin{cases} \text{sign}\,(\lambda_{v_\theta})\ \alpha_\lambda & \text{if} \quad \alpha_\lambda \leq \alpha_{\max} \\ \\ \text{sign}\,(\lambda_{v_\theta})\ \alpha_{\max} & \text{if} \quad \alpha_\lambda > \alpha_{\max} \end{cases} \tag{11}$$

where $\alpha_\lambda \in [0,\, \pi]$ is a reference angle that depends on the local value of both $\lambda_{v_r}$ and $\lambda_{v_\theta}$, viz.

$$\alpha_\lambda \triangleq \arccos\left( \frac{\lambda_{v_r}}{\sqrt{\lambda_{v_r}^2 + \lambda_{v_\theta}^2}} \right) \tag{12}$$

Also, because $\mathcal{H}$ depends linearly on $\tau$, a bang-bang control law for the switching parameter is optimal, that is:

$$\tau = \begin{cases} 0 & \text{if} \quad (\lambda_{v_r}\, \cos\alpha + \lambda_{v_\theta}\, \sin\alpha) \leq 0 \\ \\ 1 & \text{if} \quad (\lambda_{v_r}\, \cos\alpha + \lambda_{v_\theta}\, \sin\alpha) > 0 \end{cases} \tag{13}$$

where $\alpha$ is now given by Eq. (11). Recalling that the only constraint is the final distance $r_f$,

the boundary conditions at the end of the transfer are:

$$r(t_f) = r_f \quad , \quad \lambda_\theta(t_f) = 0 \quad , \quad \lambda_{v_r}(t_f) = 0 \quad , \quad \lambda_{v_\theta}(t_f) = 0 \tag{14}$$

In other terms, the spacecraft final angular position $\theta(t_f)$ and its velocity components $v_r(t_f)$ and $v_\theta(t_f)$ are left free and are outputs of the optimization process. Finally, the minimum flight time is obtained by enforcing the transversality condition $\mathcal{H}(t_f) = 1$, see Ref. [18].

To summarize, the spacecraft motion is described by the four equations of motion (1)–(4) and the four Euler-Lagrange equations (7)–(10). This differential system is completed with eight boundary conditions, four of which are given by Eqs. (5) and the remaining four are given by Eqs. (14).

## 3 Nodal Flyby Missions with Near-Earth Asteroids

The analysis of nodal missions to NEAs can be divided into two succeeding phases. Firstly, the previous mathematical model has been used to obtain, in a parametric form, the minimum flight time $t_f$ as a function of both the heliocentric distance ($r_f$) to be reached, and the spacecraft characteristic acceleration ($a_c$). The target distance has been varied within the range $r_f \in [0.2,\, 12]$ au to include all possible mission scenarios. The lower limit of such a distance range has been included mainly for the sake of completeness. In fact, it is necessary to guarantee that the spacecraft distance be always greater than a minimum value based on thermal and mechanical constraints involving the E-sail tethers. This minimum value is estimated to be between 0.33 au (assuming copper tethers) and 0.5 au (using aluminum tethers) [14]. In addition, the parametric analysis has been conducted assuming a spacecraft characteristic acceleration ranging within the interval $a_c \in [0.5,\, 1.5]\,\mathrm{mm/s^2}$. The actual value of $a_c$, which defines the propulsive capabilities of an E-sail, depends on the overall dimensions of the spacecraft and on the onboard payload mass. A mathematical model useful for estimating the spacecraft

characteristic acceleration is discussed in Ref. [19]. For example, a characteristic acceleration of $1\,\mathrm{mm/s^2}$ corresponds to a total spacecraft mass of about 391 kg, with a payload mass of 100 kg.

The results of this first phase of study have been summarized in Fig. 3, which is divided into two parts to highlight transfers toward inner zones (with $r_f < 1\,\mathrm{au}$, see Fig. 3(a)) and outer zones ($r_f > 1\,\mathrm{au}$, see Fig. 3(b)) of the interplanetary space. Figure 4 shows two typical transfer trajectories with $r_f < 1\,\mathrm{au}$ (Fig. 4(a)) and $r_f > 1\,\mathrm{au}$ (Fig. 4(b)) for an E-sail with $a_c = 1\,\mathrm{mm/s^2}$. In other terms Fig. 3 shows the isocontour curves of the surface $t_f = t_f(r_f, a_c)$, which has been obtained numerically.

Transfers toward distances with $r_f > 1\,\mathrm{au}$ may actually experience two different types of optimal trajectories. In fact, for sufficiently high values of $a_c$, the minimum-time trajectory corresponds to a direct transfer (DT), that is, a trajectory that increases, at any time, the instantaneous Sun-spacecraft distance. In some cases, that is, when the E-sail experiences a modest characteristic acceleration and for high values of distances to be reached, the optimal trajectory has a different structure. Initially the spacecraft decreases its distance from the Sun to fully exploit the increase of propulsive acceleration resulting from the growing solar wind electron density and temperature. Such a behavior is referred to as solar wind assist (SWA) [14] and is illustrated in Fig. 5, which shows the optimal trajectory to reach a distance of 6 au using an E-sail with $a_c = 0.5\,\mathrm{mm/s^2}$. Note the remarkable difference as compared to the trajectory of Fig. 4(b), even though the final distance is the same in the two cases. In addition, the simulations show that a DT trajectory is characterized by a propulsive system that is switched on ($\tau = 1$) along the whole trajectory, while a SWA maneuver is usually preceded by a coasting phase ($\tau = 0$) whose length depends on the value of characteristic acceleration.

To summarize, for a given final distance $r_f$ to reach, there exists a critical value of spacecraft characteristic acceleration below which the required distance is more quickly obtained with a

SWA trajectory rather than with a DT. The locus of points $(t_f, r_f)$ in correspondence of which a DT and a SWA transfer require the same mission time for a given value of $a_c$ have been highlighted in Fig. 3(b) with a dashed line.

The type of optimal trajectory (that is, DT or SWA) cannot be predicted in advance, that is, for a given pair $(r_f, a_c)$ it is not possible to state if the optimal trajectory will include or not a SWA. The answer can only be obtained by simulation. Indeed an indirect approach to a variational problem is known to provide only necessary conditions to the solutions. As a result, for a given pair $(r_f, a_c)$ it is possible that both a DT and a SWA satisfy the boundary conditions and the transversality condition. For this reason, the shape of the boundary region that separates a DT from a SWA (dotted line in Fig. 3(b)) has been found numerically. In addition, these results are useful for the succeeding analysis of nodal flyby, to be discussed now.

In the second part of this analysis, a number of flyby missions toward NEAs have been simulated. Data regarding the whole set $\mathcal{J}$ of 9546 known NEAs, calculated at mid January 2013, have been retrieved from the JPL database [1]. Using the solar distances of both orbital nodes of each asteroid in the set $\mathcal{J}$, the corresponding minimum time trajectory required to attain a nodal flyby has been calculated. The previous analysis regarding the combinations of mission time, solar distance and spacecraft characteristic acceleration is useful for identifying both the correct solution of the optimal problem in terms of either SWA trajectory or direct transfer, and for providing a first guess of the unknowns (that is, the initial adjoint variables and the transfer time). Using such an approach, about 19000 optimal trajectories have been analyzed for an E-sail-based spacecraft with a characteristic acceleration $a_c = 1\,\mathrm{mm/s^2}$. The simulation results, including the minimum flight time and the polar angle $\Delta\theta$ swept by the spacecraft along the whole transfer trajectory, have been collected in a database attached to this paper

[1] `http://neo.jpl.nasa.gov/cgi-bin/neo_elem` (retrieved at January 15, 2013)

as electronic supplementary material. An excerpt of the obtained results is shown in Table 2. Note, for example, that the optimal transfer toward the ascending node of Icarus (Id 6 of Table 2) has not been calculated because its distance from the Sun is lower than 0.2 au. In fact, as discussed above, such a distance would correspond to an excessive spacecraft temperature.

Figure 6 summarizes the performance of an E-sail, showing the required minimum mission times necessary to reach a NEA in terms of cumulative percent. For each asteroid, the target node corresponds to the solution (that is, ascending or descending node) that minimizes the flight time. Figure 6 shows that over 60% of NEAs can be reached with a total flight time less than 100 days. The same figure also highlights four particularly representative asteroids. Notably, all of the NEAs can be reached with a maximum flight time of about 300 days.

## 4 Conclusions

Nodal flyby missions toward NEAs have been studied for an Electric Solar Wind Sail, a spacecraft that uses the solar wind dynamic pressure for generating a continuous propulsive thrust without the need for reaction mass. A two-dimensional simplified problem has been discussed to obtain a preliminary estimate of the performance of such a propulsion system with reasonable simulation times. Minimum-time trajectories have been studied in an optimal framework using an indirect approach. The optimal trajectory may or may not include a solar wind assist phase depending on the value of the spacecraft characteristic acceleration and on the solar distance of the node to reach. About 19000 optimal trajectories have been analyzed assuming a spacecraft characteristic acceleration of $1\,\mathrm{mm/s^2}$. The simulation results, including the minimum flight time to arrive at the nodes of each near-Earth asteroid and the polar angle swept by the spacecraft along the whole transfer, have been collected in a database. Most asteroids can be reached within reasonable mission times, and over 60% of NEA population requires a total mission time less than 100 days. The obtained results have been obtained using a simplified

model that provides a reasonable estimate of the absolute minimum mission time. This information is of great practical importance. In fact it allows the designer to preliminarily prune a large set of possible asteroids and reduce the number of feasible targets. It also quantifies the sensitivity of the mission time with respect to the Electric Solar Wind Sail performance (in terms of characteristic acceleration) and, as such, it defines the minimum technology level necessary to reach a given target within a tolerable flight time.

## Acknowledgments

This research has been financed in part within the European Community's Seventh Framework Programme ([FP7/2007-2013]) under grant agreement number 262733.

## References

[1] D. Perna, M. Barucci, M. Fulchignoni, The near-earth objects and their potential threat to our planet, The Astronomy and Astrophysics Review 21 (1) (2013) 1–28, doi: 10.1007/s00159-013-0065-4.

[2] T. J. McCoy, M. S. Robinson, L. R. Nittler, T. H. Burbine, The near earth asteroid rendezvous mission to asteroid 433 eros: A milestone in the study of asteroids and their relationship to meteorites, Chemie der Erde - Geochemistry 62 (2) (2002) 89 – 121, doi: 10.1078/0009-2819-00004.

[3] J. Baker, The falcon has landed, Science 312 (5778) (2006) 1327, doi: 10.1126/science.312.5778.1327.

[4] M. Barucci, E. Dotto, A. Levasseur-Regourd, Space missions to small bodies: asteroids and cometary nuclei, Astronomy and Astrophysics Review 19 (1) (2011) 1–29, doi: 10.1007/s00159-011-0048-2.

[5] J. González, M. Belló, J. Martín-Albo, A. Gílvez, Don Quijote: An ESA mission for the assessment of the NEO threat, in: 55th International Astronautical Congress 2004, Vol. 10, International Astronautical Federation, 2004, pp. 6605–6613.

[6] M. A. Barucci, et al., MARCO POLO near-earth asteroid sample return mission, Assessment Study Report ESA/SRE(2009)3, ESA (December 2009), available online (cited February 3rd, 2014) http://sci.esa.int/science-e/www/object/index.cfm?fobjectid=46019.

[7] P. Michel, M. Barucci, A. Cheng, H. Böhnhardt, J. Brucato, E. Dotto, P. Ehrenfreund, I. Franchi, S. Green, L.-M. Lara, B. Marty, D. Koschny, D. Agnolon, Marcopolo-r: Near-earth asteroid sample return mission selected for the assessment study phase of the ESA program cosmic vision, Acta Astronautica 93 (0) (2014) 530–538, doi: 10.1016/j.actaastro.2012.05.030.

[8] J. Bottke W.F., R. Jedicke, A. Morbidelli, J.-M. Petit, B. Gladman, Understanding the distribution of near-earth asteroids, Science 288 (5474) (2000) 2190–2194, doi: 10.1126/science.288.5474.2190.

[9] M. Granvik, J. Vaubaillon, R. Jedicke, The population of natural earth satellites, Icarus 218 (1) (2012) 262–277, doi: 10.1016/j.icarus.2011.12.003.

[10] E. Perozzi, A. Rossi, G. B. Valsecchi, Basic targeting strategies for rendezvous and flyby missions to the near-earth asteroids, Planetary and Space Science 49 (1) (2001) 3–22, doi: 10.1016/S0032-0633(00)00124-0.

[11] G. W. Hughes, C. R. McInnes, Small-body encounters using solar sail propulsion, Journal of Spacecraft and Rockets 41 (1) (2004) 140–150, doi: 10.2514/1.9277.

[12] P. Janhunen, P. K. Toivanen, J. Polkko, S. Merikallio, P. Salminen, E. Haeggstrom, H. Seppanen, R. Kurppa, J. Ukkonen, S. Kiprich, G. Thornell, H. Kratz, L. Richter, O. Kromer, R. Rosta, M. Noorma, J. Envall, S. Latt, G. Mengali, A. A. Quarta, H. Koivisto, O. Tarvainen, T. Kalvas, J. Kauppinen, A. Nuottajarvi, A. Obraztsov, Electric solar wind sail: Towards test missions, Review of Scientific Instruments 81 (11) (2010) 111301 (1–11), doi: 10.1063/1.3514548.
URL http://link.aip.org/link/?RSI/81/111301/1

[13] P. Janhunen, Electric sail for spacecraft propulsion, Journal of Propulsion and Power 20 (4) (2004) 763–764, doi: 10.2514/1.8580.

[14] A. A. Quarta, G. Mengali, Electric sail mission analysis for outer solar system exploration, Journal of Guidance, Control, and Dynamics 33 (3) (2010) 740–755, doi: 10.2514/1.47006.

[15] A. A. Quarta, G. Mengali, Electric sail missions to potentially hazardous asteroids, Acta Astronautica 66 (9-10) (2010) 1506–1519, doi: 10.1016/j.actaastro.2009.11.021.

[16] G. Mengali, A. A. Quarta, G. Aliasi, A graphical approach to electric sail mission design with radial thrust, Acta Astronautica 82 (2) (2013) 197–208, doi: 10.1016/j.actaastro.2012.03.022.

[17] A. A. Quarta, G. Mengali, P. Janhunen, Optimal interplanetary rendezvous combining electric sail and high thrust propulsion system, Acta Astronautica 68 (5-6) (2011) 603–621, doi: 10.1016/j.actaastro.2010.01.024.

[18] A. E. Bryson, Y. C. Ho, Applied Optimal Control, Hemisphere Publishing Corporation, New York, NY, 1975, Ch. 2, pp. 71–89, ISBN: 0-891-16228-3.

[19] P. Janhunen, A. A. Quarta, G. Mengali, Electric solar wind sail mass budget model, Geoscientific Instrumentation, Methods and Data Systems 2 (1) (2013) 85–95, doi: 10.5194/gi-2-85-2013.

**List of Tables**

| $r_f$ [au] | 0.4 | 0.5 | 0.6 | 0.7 | 0.8 | 0.9 | 2 | 3 | 4 | 5 | 8 | 10 | 12 |
|---|---|---|---|---|---|---|---|---|---|---|---|---|---|
| $\bar{t}_f$ [days] | 234 | 222 | 209 | 194 | 176 | 151 | 207 | 330 | 444 | 551 | 843 | 1022 | 1192 |

Table 1
Value of $\bar{t}_f$ as a function of the distance $r_f$, for an E-sail with $a_c = 1$ mm/s$^2$.

| | | Descending Node | | | Ascending Node | | |
|---|---|---|---|---|---|---|---|
| Id | Name | $r_f$ [au] | $\Delta\theta$ [deg] | $t_f$ [days] | $r_f$ [au] | $\Delta\theta$ [deg] | $t_f$ [days] |
| 1 | 433 Eros (1898 DQ) | 1,1335 | 65,8856 | 69,33 | 1,7823 | 130,2887 | 177,8429 |
| 2 | 719 Albert (1911 MT) | 1,2154 | 80,6579 | 87,823 | 3,6821 | 179,097 | 408,7889 |
| 3 | 887 Alinda (1918 DB) | 3,8124 | 180,706 | 423,33 | 1,0768 | 51,6046 | 53,1307 |
| 4 | 1036 Ganymed (1924 TD) | 1,3981 | 102,8209 | 120,89 | 2,9788 | 168,1276 | 328,0322 |
| 5 | 1221 Amor (1932 EA1) | 2,546 | 158,5202 | 276,1 | 1,1193 | 62,7493 | 65,6545 |
| 6 | 1566 Icarus (1949 MA) | 1,1603 | 71,2667 | 75,822 | 0,1998 | × | × |
| 7 | 1580 Betulia (1950 KA) | 1,1483 | 68,9397 | 72,984 | 3,0818 | 170,0316 | 340,1202 |
| 8 | 1620 Geographos (1951 RA) | 1,151 | 69,4866 | 73,647 | 1,0629 | 47,1171 | 48,2819 |
| 9 | 1627 Ivar (1929 SH) | 1,1308 | 65,2998 | 68,638 | 2,5633 | 158,9632 | 278,2145 |
| 10 | 1685 Toro (1948 OA) | 0,8766 | 144,4255 | 158,1 | 1,5027 | 112,0384 | 137,4491 |

Table 2
Simulation results obtained for sample NEAs with $a_c = 1$ mm/s$^2$ (excerpt).

**List of Figures**

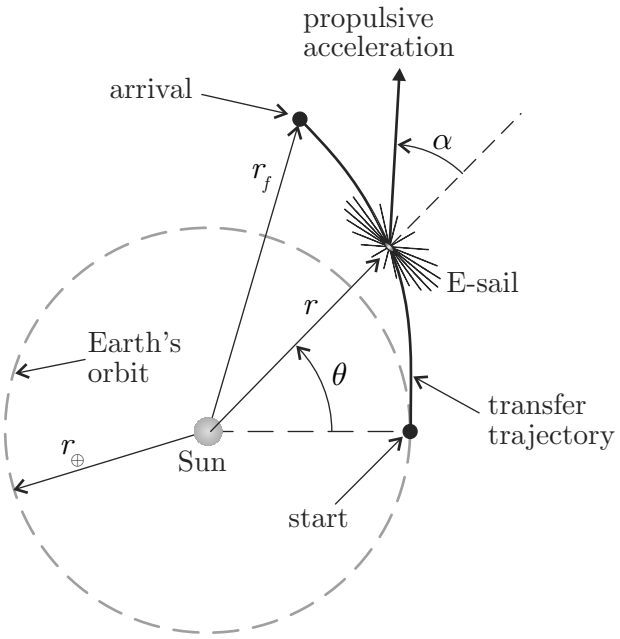


Figure 1. Reference frame and E-sail cone angle.

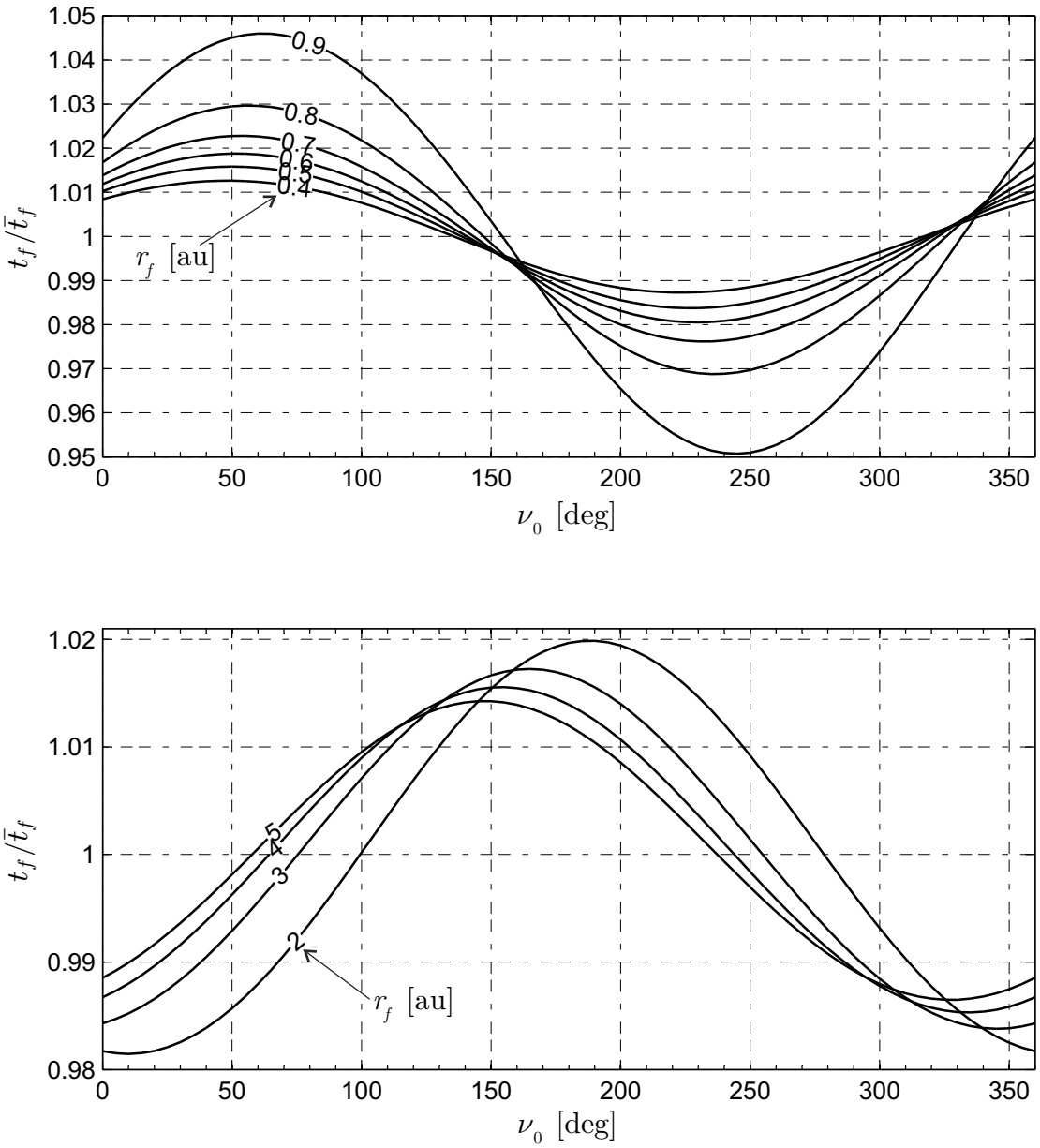


Figure 2. Minimum flight time $t_f$ as a function of $r_f$ and the starting true anomaly $\nu_0$, for an E-sail with $a_c = 1$ mm/s$^2$.

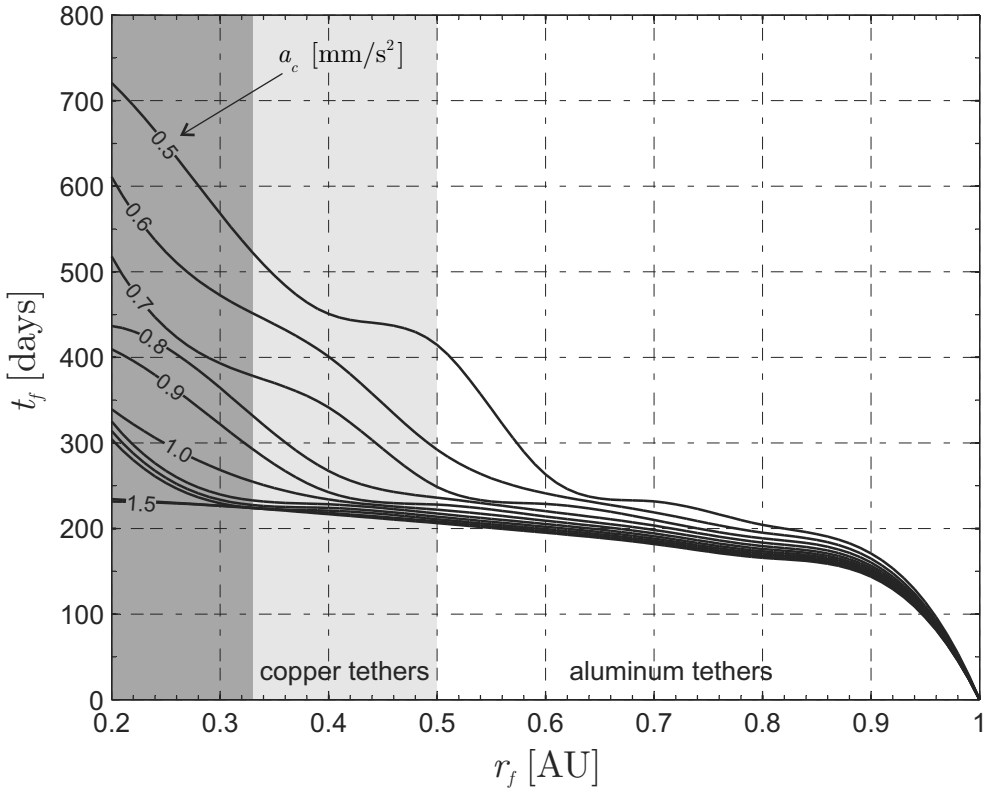


(a) Nodes with $r_f < 1\,\mathrm{au}$

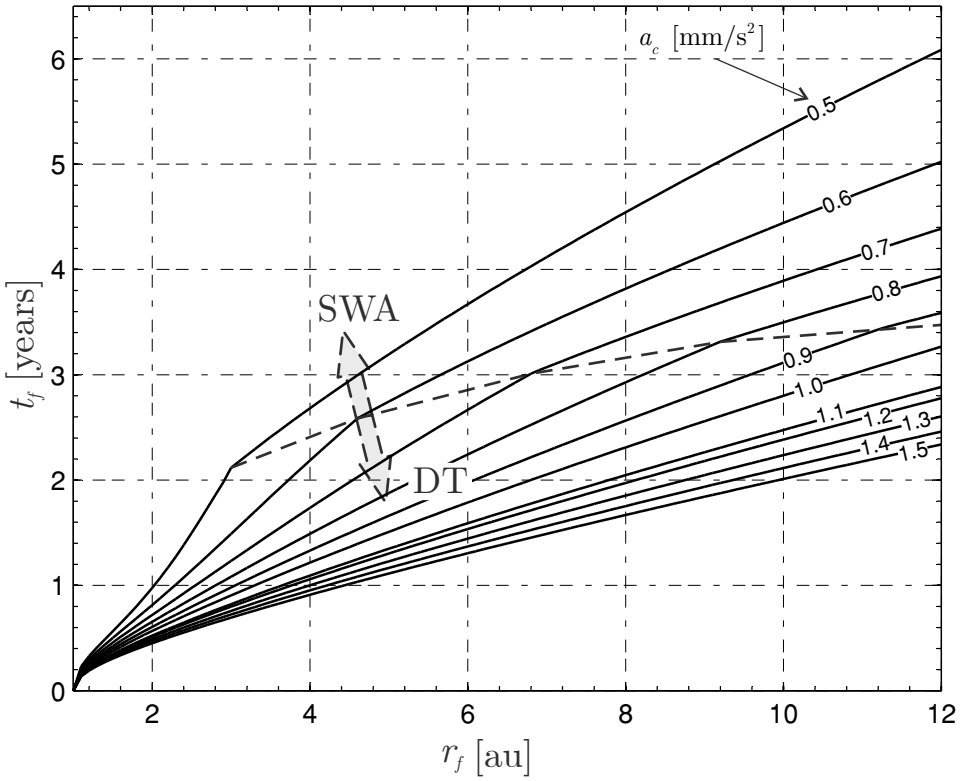


(b) Nodes with $r_f > 1\,\mathrm{au}$

Figure 3. Minimum flight time $t_f$ as a function of $r_f$ and $a_c$.

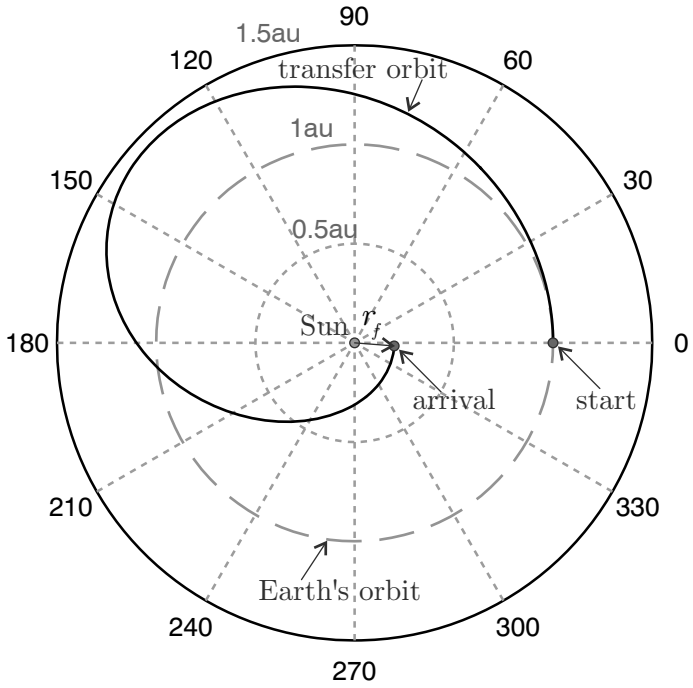


(a) $r_f = 0.2\,\mathrm{au}$

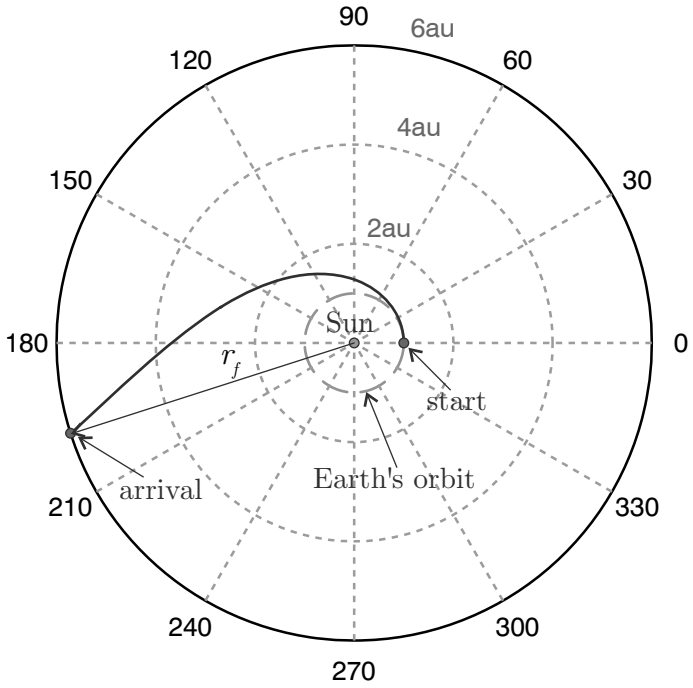


(b) $r_f = 6\,\mathrm{au}$

Figure 4. Optimal transfer trajectory for an E-sail with $a_c = 1\ \mathrm{mm/s^2}$.

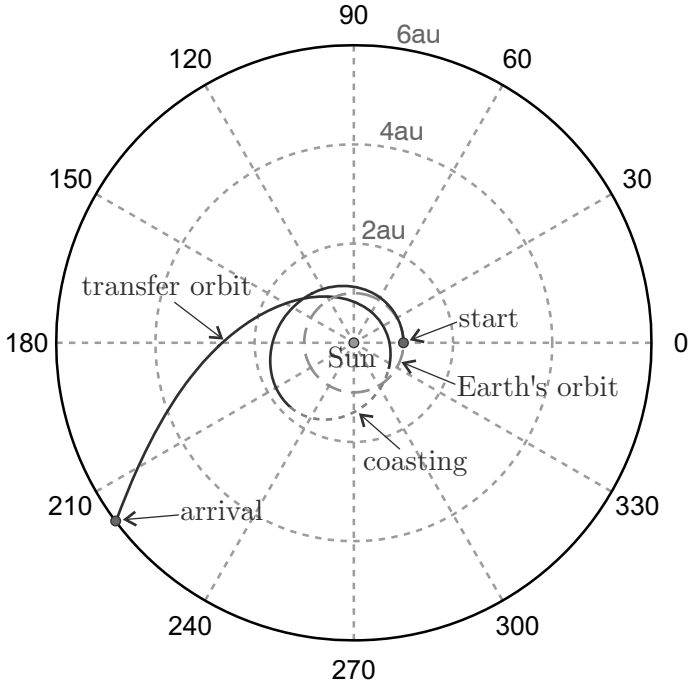


Figure 5. Optimal transfer trajectory with a SWA ($a_c = 0.5$ mm/s$^2$ and $r_f = 6$ au).

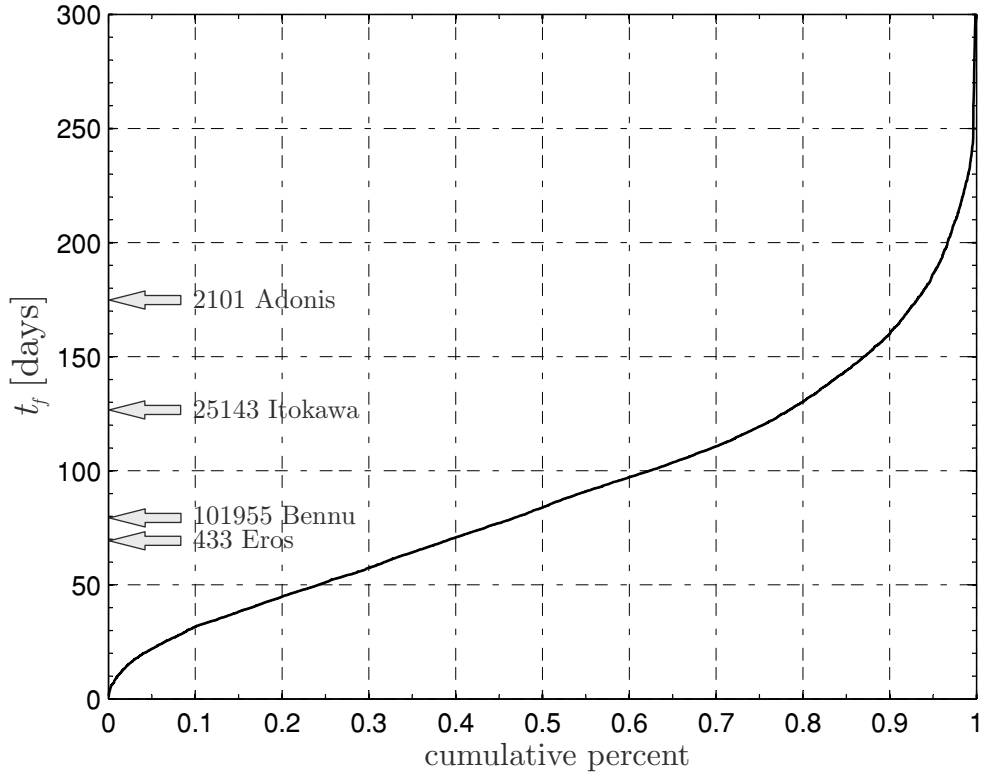


Figure 6. Performance of an Earth-NEA optimum E-sail transfer ($a_c = 1$ mm/s$^2$).